Frontiers in Bioscience Landmark

Front. Biosci. (Landmark Ed) **2025**; 30(10): 45595
https://doi.org/10.31083/FBL45595

Original Research

Astragalus Polysaccharide Improves Myocardial Fibrosis in Hypertrophic Cardiomyopathy Through the TGF-β_1/Smad3 Signal Pathway

Nana Qin[1,†], Wenjun Wu[2,†], Baoyin Li[1,*]

[1]State Key Laboratory of Frigid Zone Cardiovascular Disease, Department of Cardiovascular Surgery, General Hospital of Northern Theater Command, 110016 Shenyang, Liaoning, China
[2]Graduate School of Changchun University of Chinese Medicine, 130117 Jilin, Jilin, China
*Correspondence: 982850299@qq.com (Baoyin Li)
[†]These authors contributed equally.

Academic Editor: Natascia Tiso
Submitted: 6 August 2025 Revised: 13 October 2025 Accepted: 17 October 2025 Published: 29 October 2025

Abstract

Background: Myocardial fibrosis is a key pathological driver of Hypertrophic Cardiomyopathy (HCM), contributing to adverse remodeling and poor prognosis. The transforming growth factor-β_1/Smad3 (TGF-β_1/Smad3) signaling cascade plays a central role in fibrogenesis; however, effective antifibrotic therapies remain limited. *Astragalus polysaccharide* (APS), a bioactive constituent of *Astragalus membranaceus*, has demonstrated cardioprotective potential. Nevertheless, the mechanisms underlying its effects in HCM-associated fibrosis remain unknown. **Methods**: Pressure overload induced HCM was established in C57BL/6J mice using transverse aortic constriction (TAC), and animals were randomized to control, TAC, low-dose APS (50 mg/kg/day), or high-dose APS (100 mg/kg/day) groups. Cardiac function was evaluated by echocardiography, while myocardial hypertrophy and fibrosis were assessed by morphometry, Masson's staining, and collagen I (Col-I) expression analysis. Parallel *in vitro* studies employed angiotensin II stimulated (Ang II-stimulated) H9C2 cardiomyocytes, with or without the TGF-β_1/Smad3 agonist SRI-011381, to explore mechanistic pathways. **Results**: TAC induced marked cardiac dysfunction, ventricular dilation, and extensive fibrosis, accompanied by upregulation of TGF-β_1, phosphorylated Smad3, and Col-I expression (all $p < 0.05$). APS treatment dose-dependently preserved systolic function, attenuated collagen deposition, and suppressed activation of the TGF-β_1/Smad3 axis, with the strongest effects observed in the high-dose group. *In vitro*, APS significantly inhibited Ang II induced hypertrophy and fibrotic protein expression; these effects were abrogated by SRI-011381, confirming pathway specificity. **Conclusions**: APS exerts cardioprotective and antifibrotic effects in HCM by inhibiting the TGF-β_1/Smad3 signaling pathway. These findings highlight APS as a promising therapeutic candidate for targeting myocardial fibrosis and improving outcomes in HCM.

Keywords: *Astragalus polysaccharides*; hypertrophic cardiomyopathy; myocardial fibrosis; TGF-β_1/Smad3 signal

1. Introduction

Hypertrophic Cardiomyopathy (HCM) is a common hereditary cardiovascular disease characterized by the thickening of the ventricular walls, particularly in the interventricular septum [1,2]. Clinically, HCM manifests in a variety of ways, including palpitations, chest pain, shortness of breath, and syncope, with severe cases leading to heart failure or sudden cardiac death [3,4]. Thus, there is an urgent need to develop effective antifibrotic strategies clinical. Transforming growth factor-β_1 (TGF-β_1) plays a crucial role in inflammation, cell proliferation, and tissue repair. Sustained activation of TGF-β_1 induces fibroblast proliferation and excessive extracellular matrix (ECM) deposition. In addition, its overexpression has been strongly associated with multiple fibrotic disorders, exhibiting a positive correlation with disease severity [5,6]. *Astragalus membranaceus*, a widely used traditional Chinese medicinal herb, exerts broad cardiovascular protective effects, Inflammatory factors such as TNF-α promote fibroblast proliferation and collagen synthesis through the TGF-β/Smad pathway, leading to excessive myocardial fibrosis. This fibrosis not only diminishes cardiac contractile function but also increases myocardial stiffness, impairing effective blood pumping. It reduces atrial conduction velocity and contributes to structural and electrophysiological remodeling of the atria, thereby facilitating the initiation and maintenance of HCM [7]. Among its bioactive constituents, *Astragalus polysaccharide* (APS) exhibits anti-inflammatory, antioxidant, and cardioprotective properties [8,9]. Notably, APS ameliorates diabetic cardiomyopathy and improves impaired cardiac function, potentially providinge multifaceted cardioprotection [10].

In this study, we employed a transverse aortic constriction (TAC) model to induce HCM in mice and an angiotensin II-induced (Ang II-induced) hypertrophy model in cardiomyoceytes to investigate the regulatory effects of APS on the classical TGF-β_1/Smad3 fibrosis signaling pathway. By using APS as an intervention, we aimed to ex-

plore the mechanisms underlying its effects in modulating myocardial fibrosis and provide experimental evidence and theoretical insights into its potential therapeutic application in HCM.

2. Materials and Methods

2.1 Establishment of the TAC-Induced HCM Model

Male C57BL/6J mice were provided by Beijing Huafukang Bioscience Co., Ltd. (Beijing, China; license number: SCXK [Jing] 2019-0008). Forty mice after 1 week of acclimatization, under anesthesia with 1% isoflurane, a 3-mm incision was made at the proximal sternum to fully expose the aortic arch. A blunt 27-gauge needle was positioned between the two carotid arteries, directly over the aortic arch. Using 7-0 silk suture, the aortic arch was ligated against the needle at a site immediately distal to the brachiocephalic artery. The needle was then promptly removed, creating a reproducible TAC. Following the procedure, the sternum and skin were closed with 6-0 polypropylene sutures, and the mice were placed on a pre-warmed heating pad until full recovery from anesthesia. Sham-operated animals underwent the identical surgical exposure without aortic ligation. Beginning on postoperative day 2, the drug concentration is based on previous literature [11,12], mice assigned to the high-dose group (APS-H) and low-dose group (APS-L) received intragastric administration of APS at 50 mg/kg/day and 100 mg/kg/day, respectively (APS: Solarbio, China, cat. no.AGV 7970, purity $\geq$90%); the remaining groups received an equivalent volume of purified water. Treatment continued for 4 consecutive weeks. At 4 weeks post-surgery, mice were re-anesthetized using a precision gas anesthesia system, with isoflurane concentration titrated to 2.5% $\pm$ 0.5% for induction and maintained at 1.8% $\pm$ 0.3% for imaging, while oxygen flow was maintained at 1 L/min. Following transthoracic echocardiographic assessment, animals were euthanized via cervical dislocation. Freshly excised hearts were immediately weighed and processed for downstream analyses, including histopathology and western blotting.

2.2 Echocardiographic Assessment

At 4 weeks post-surgery, cardiac function was assessed using a high-resolution small-animal ultrasound system (The manufacturers and production addresses of the equipment used are listed in Table 1). Measured parameters included left ventricular ejection fraction (LVEF), left ventricular fractional shortening (LVFS), left ventricular end-diastolic internal diameter (LVIDd), left ventricular end-systolic internal diameter (LVIDs), left atrial diameter (LAD), and left atrial diastolic area (LA diastolic area).

2.3 Histopathological Analysis

Cardiac tissues were paraffin-embedded, sectioned, and subjected to Masson's trichrome staining according to the instructions provided by the manufacturer's instructions (The manufacturers, production addresses, and batch numbers of the kits used are shown in Table 1). Images were acquired using an upright microscope under identical settings (magnification: $\times$20). For each animal, at least three sections were analyzed, and 5–10 random fields per section were selected. ImageJ software (Wayne Rasband and contributors National Institutes of Health, USA, Java 1.8.0 345, http://imagej.org) was used to separate the color channels, and a uniform threshold for the collagen-positive blue channel was set based on control and positive reference samples. Batch processing was applied to all images.

2.4 Immunohistochemistry

Paraffin-embedded sections were subjected to deparaffinization, hydration, and antigen retrieval before immunohistochemical staining, which was carried out using a commercially available kit (The manufacturers, production addresses, and batch numbers of the kits used are shown in Table 1). Expression of collagen I (Col-I) was detected under a light microscope, and quantitative evaluation was subsequently performed.

2.5 Immunofluorescence

Cardiac sections were first fixed and permeabilized, then blocked with 5% bovine serum albumin. After overnight exposure to anti-Col-I antibodies, samples were incubated with fluorophore-conjugated secondary antibodies and counterstained with DAPI. Fluorescence images were acquired under identical conditions at $\times$40 magnification. The average signal intensity was measured using ImageJ, normalized to myocardial area, and the percentage of positive area was compared with the control group (The manufacturers, batch numbers, and preparation ratios of the antibodies used are shown in Table 1).

2.6 H9C2 Hypertrophy Model

H9C2 rat cardiomyoblasts (ATCC® CRL-1446™) were obtained from ATCC (Manassas, VA, USA). Cell lines were authenticated by short tandem repeat profiling, regularly screened for mycoplasma contamination with the MycoAlert™ kit (Lonza, Switzerland), and cross-referenced with ICLAC and Cellosaurus databases. Cells were maintained in high-glucose DMEM supplemented with 10% fetal bovine serum and 1% penicillin–streptomycin. After reaching ~50–60% confluence, cultures were serum-deprived for 24 h. Hypertrophy was induced by Ang II (1×10^{-5} mmol/L) for 24 h. To examine the involvement of TGF-β_1/Smad3 signaling, cells were exposed to the agonist SRI-011381 (10 µM), either alone or in combination with APS (600 µg/mL).

2.7 Cell Counting Kit-8 (CCK8)

Cells were seeded into 96-well plates and incubated for 24 hours (1×10^4 cells per well), followed by treatment with varying concentrations of Ang II for an addi-

Table 1. Related consumables and companies.

Reagent/Instrument name	Technology (cat. no)
Bovine serum albumin	Lanjieko Technology, Beijing, China
PMSF (100 Mm)	Beyotime, Shanghai, China
5×sodium dodecyl sulfate-polyacrylamide gel electrophoresis	Beyotime, Shanghai, China
Enhanced chemiluminescence	NCM Biotech, Suzhou, China
Astragalus polysaccharides	AGV 7970, Solarbio, Beijing, China
Non-fat milk	Yili Global, Inner Mongolia, China
TEMED	Shanghai, China
Masson's trichrome staining	abs9347, Absin, Shanghai, China
Commercial immunohistochemical kit	Kaiji, Shanghai, China (KGC3201-300)
Dulbecco's modified Eagle's medium	Sevicebio, Wuhan, China
1% penicillin–streptomycin	Thermo Fisher, Shanghai, China
Fetal bovine serum	Thermo Fisher, Shanghai, China
4',6-diamidino-2-phenylindole	Beyotime, Shanghai, China
Cell Counting Kit-8	C0038, Beyotime, Shanghai, China
SRI-011381	1629138-41-5, MedChemExpress, Princeton, NJ, USA
Collagen I Antibody (mouse)	1:1000, sc-59772, Santa, Shanghai, China
TGF-β Antibody (mouse)	1:1000, sc-130348, Santa, Shanghai, China
Smad3 (rabbit)	1:1000, 9523, Cell Signaling Technology, Danvers, MA, USA
p-Smad3 (rabbit)	1:1000, 9520, Cell Signaling Technology, Danvers, MA, USA
α-Tubulin (rabbit)	1:1000, 2144, Cell Signaling Technology, Danvers, MA, USA
Upright microscope	Chongqing UPO Optoelectronic Technology Co., Ltd., Chongqing, China
Fluorescence microscopy	Nikon, Beijing, China
High-resolution small-animal ultrasound system	VINNO Corporation, Suzhou, China
Precision gas anesthesia system	MIDMARK, Versailles, OH, USA

tional 24 hours. Subsequently, 10 µL of CCK-8 solution was added to each well and incubated in the incubator for 2 hours. Absorbance was then measured at 450 nm using a dual-wavelength method, and the data were analyzed with GraphPad Prism 8.4.0 (GraphPad Software Inc., San Diego, CA, USA).

2.8 Western Blotting

Proteins were extracted from ventricular tissues or cultured cells, quantified, and separated by SDS-PAGE. After transfer onto PVDF membranes, blocking was performed with 5% non-fat milk. Membranes were incubated with primary antibodies overnight, followed by HRP-conjugated secondary antibodies (The manufacturers, batch numbers, and preparation ratios of the antibodies used are shown in Table 1). Protein bands were visualized using enhanced chemiluminescence and analyzed with ImageJ software.

2.9 Statistical Analysis

Data analysis was conducted with GraphPad Prism 8.4.0 (GraphPad Software Inc., San Diego, CA, USA). One-way ANOVA followed by Tukey's multiple comparison test was applied to determine intergroup differences. A two-tailed p-value < 0.05 was considered statistically significant.

3. Results

3.1 APS Enhances Cardiac Function in TAC Mice

Four weeks after TAC surgery, compared with controls, mice displayed significant cardiac impairment. TAC mice showed marked declines in LVEF and LVFS, accompanied by enlarged LVIDd, LVIDs, LAD, and LA diastolic area, consistent with ventricular remodeling, and the heart weight/body weight (HW/BW) ratio was significantly elevated. These changes are consistent with the typical features of HCM. For example, studies have shown that the TAC model leads to a significant reduction in EF, with FS decreasing from 53.2% to 32.3%, indicating impaired cardiac contractile function [13]. In addition, TAC-induced pressure overload can trigger cardiac remodeling, manifested as ventricular wall thickening and chamber dilation. These alterations correspond well with the imaging characteristics observed in clinical HCM [14]. Administration of APS ameliorated these abnormalities in a dose-dependent manner. The APS-H exhibited notable improvements in systolic performance and reduced ventricular dilation, whereas the APS-L showed moderate but significant benefits. These findings highlight the cardioprotective action of APS against pressure overload induced dysfunction (Fig. 1A–I).

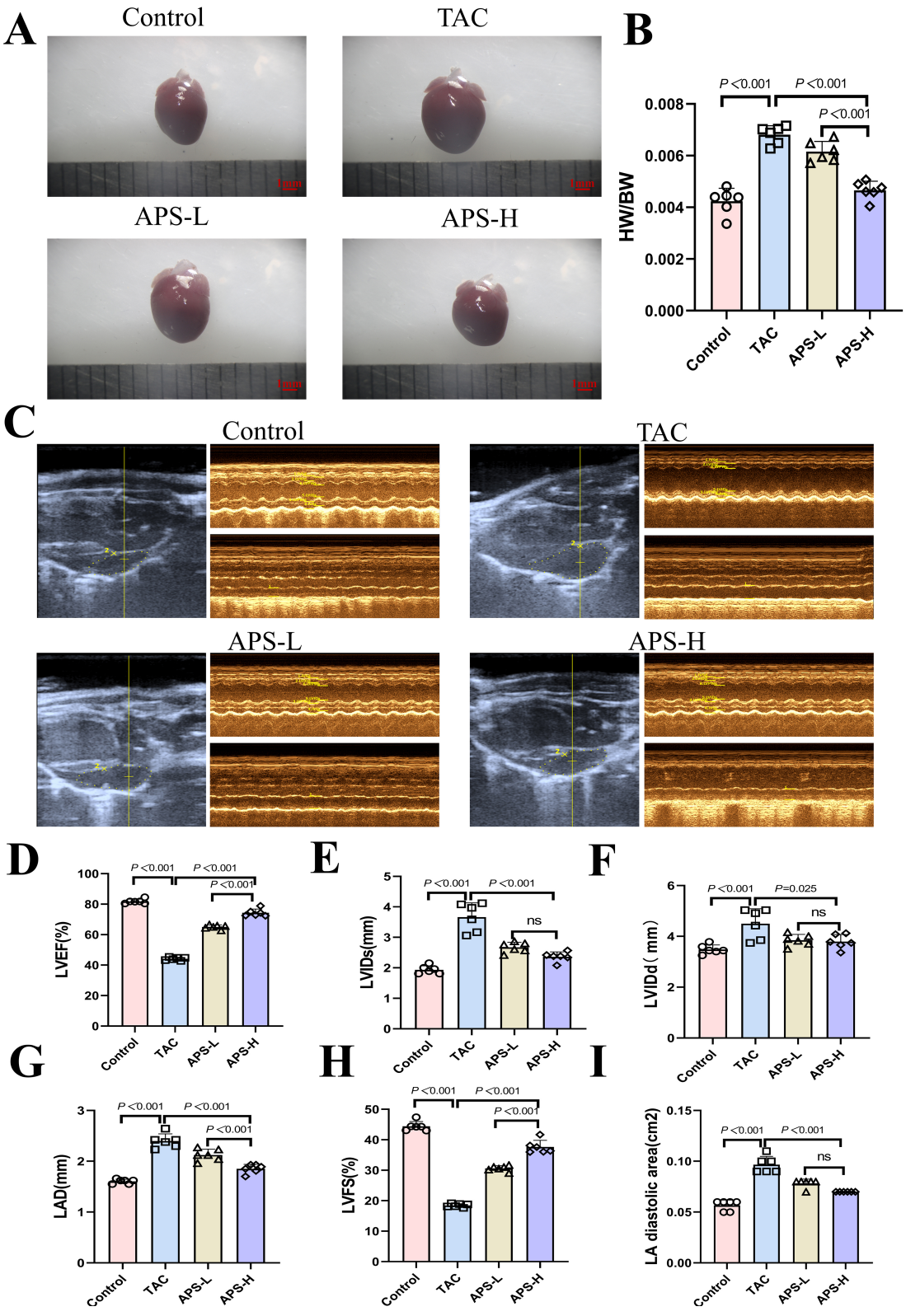

Fig. 1. ***Astragalus polysaccharide*** **(APS) improves cardiac function in transverse aortic constriction (TAC) mice.** (A) Heart photo (scale bar = 1 mm). (B) Heart weight/body weight (HW/BW). (C) Transthoracic echocardiography. (D) Left ventricular ejection fraction (LVEF). (E) End-systolic left ventricular diameter (LVIDs). (F) Eend-diastolic left ventricular diameter (LVIDd). (G) Mean left atrial straight diameter (LAD). (H) Left ventricular short axis shortening (LVFS). (I) Left atrial diastolic area (LA diastolic area). ns, no statistical difference. APS-L, low-dose APS, 50 mg/kg/day; APS-H, high-dose APS, 100 mg/kg/day. n = 6.

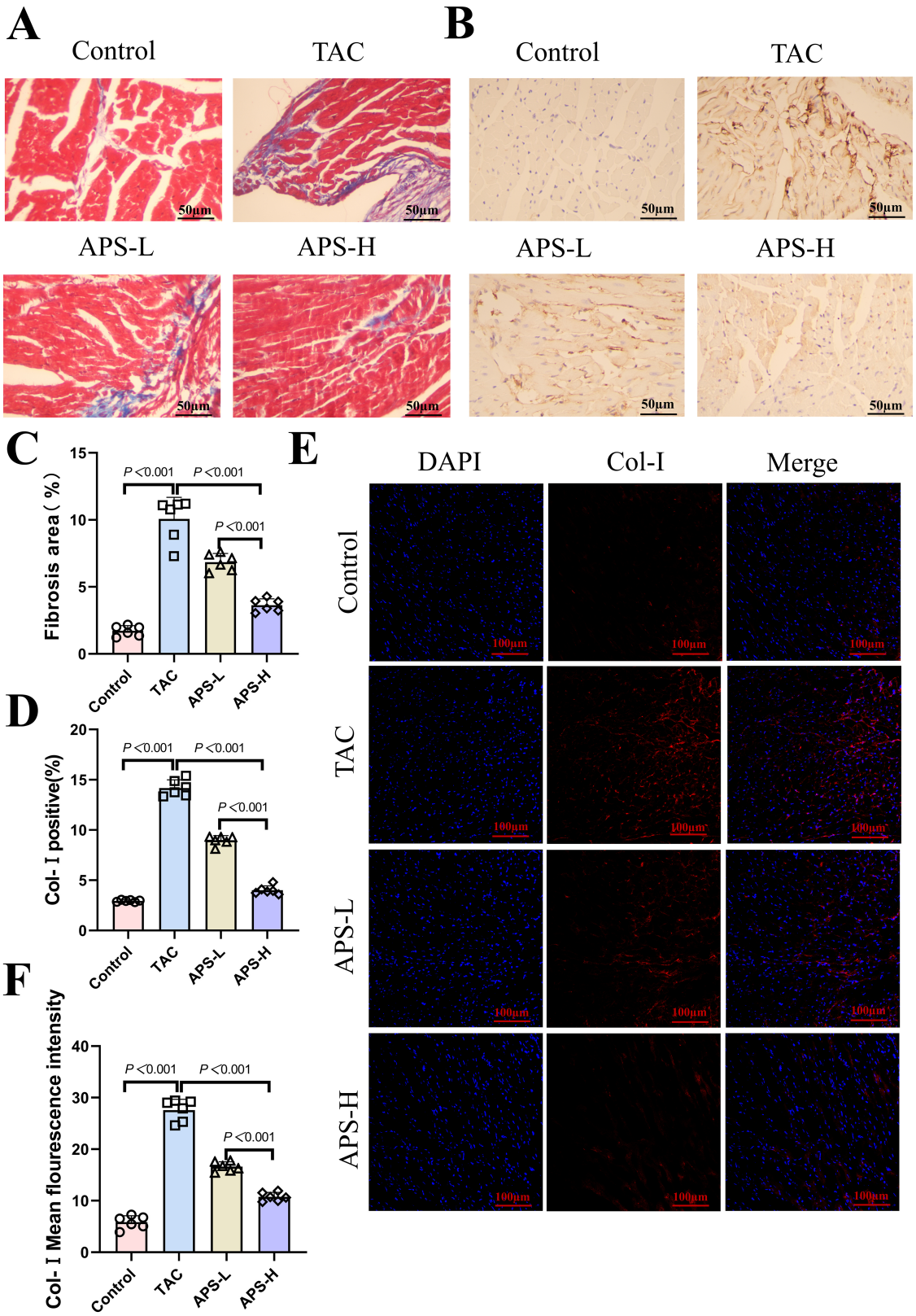

Fig. 2. APS attenuates TAC-induced myocardial fibrosis. (A) Ventricular Masson staining. (B) Collagen I (Col-I) is a representative immunohistochemical staining of the ventricle. (C) Statistical analysis of the atrial fibrosis area (scale bar = 50 μm). (D) Col-I average histochemical analysis. (E) Col-I (red) and DAPI (blue) representative ventricular immunofluorescence staining (scale bar = 100 μm). (F) Col-I average fluorescence intensity analysis. n = 6.

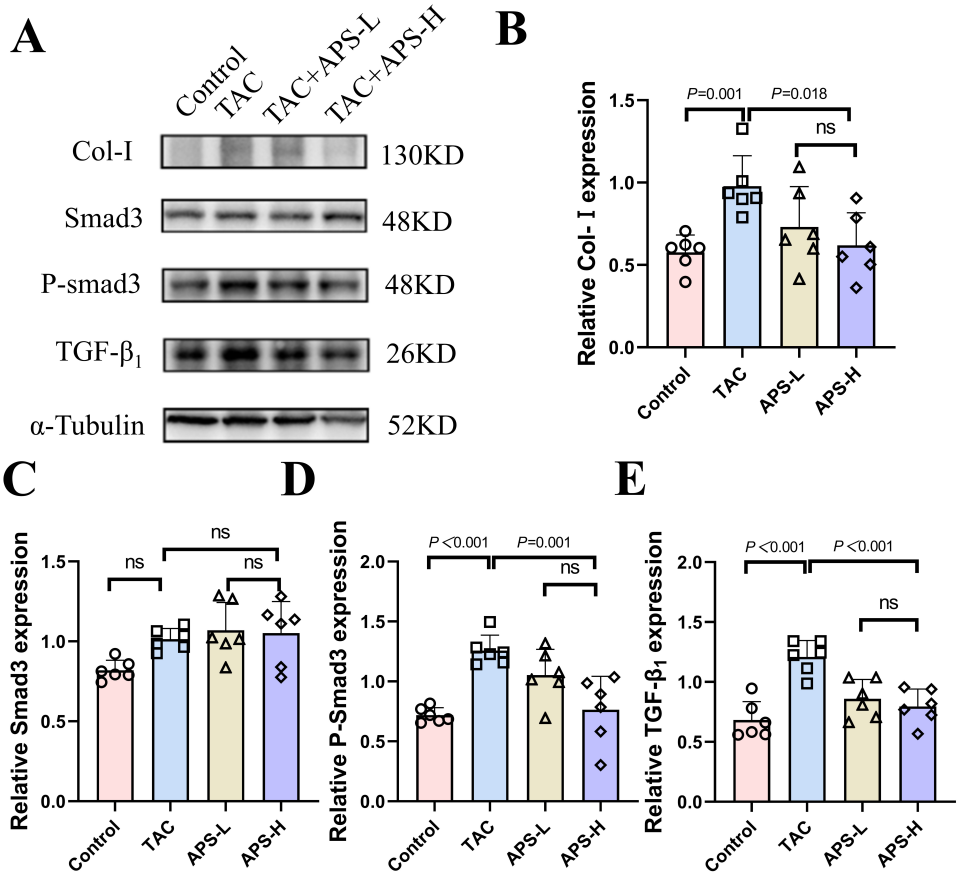

Fig. 3. APS modulates the expression of growth factor-β_1 (TGF-β_1)/Smad3 pathway-related proteins. (A) Western blotting detecting the expression of TGF-β_1, Smad3, phosphorylated Smad3 (p-Smad3), and Col-I in ventricular tissue. (B–E) Western blotting quantitative analysis. ns, no statistical difference. n = 6.

3.2 APS Attenuates Myocardial Fibrosis Triggered by TAC

Masson's staining demonstrated a robust increase in collagen accumulation in the TAC group, confirming extensive fibrotic remodeling. Quantitative analysis revealed a substantial rise in collagen volume fraction relative to controls. Treatment with APS effectively reduced collagen deposition, with the most profound suppression observed in APS-H mice. Consistently, Col-I expression, as assessed by immunohistochemistry and immunofluorescence, was significantly diminished following APS treatment, indicating its potent antifibrotic effect (Fig. 2A–F).

3.3 APS Modulates Fibrosis-Related Proteins in the TGF-β_1/Smad3 Axis

Western blot analysis revealed that TAC-induced remodeling was associated with increased myocardial expression of TGF-β_1, phosphorylated Smad3 (p-Smad3), and Col-I, while total Smad3 remained unchanged. APS administration markedly suppressed TGF-β_1 and p-Smad3 levels, along with Col-I expression. The reduction was most pronounced in APS-H animals, suggesting that APS exerts its antifibrotic activity largely through inhibition of TGF-β_1/Smad3 signaling (Fig. 3A–E).

3.4 APS Suppresses Ang II–Induced Hypertrophy in H9C2 Cells

With increasing concentrations of Ang II, cell viability decreased significantly. At 10^{-5} mmol/L, cell viability was approximately 70% of the control, which is commonly used as the experimental concentration; at 10^{-4} mmol/L, notable cell damage occurred, indicating potential toxicity. Therefore, 10^{-5} mmol/L was selected for subsequent experiments (Fig. 4A). Exposure of H9C2 cardiomyocytes to Ang II markedly upregulated the expression of TGF-β_1, p-Smad3, and Col-I, whereas co-treatment with APS attenuated these changes. APS alone had no detectable effect under basal conditions (Fig. 4B–F). Ang II treatment also significantly increased cell size, confirming successful induction of a hypertrophic phenotype, while APS treatment partially reduced cell size (Fig. 4G,H). Immunofluorescence further confirmed the downregulation of Col-I in the APS-treated group, reinforcing its role in counteracting Ang II–induced fibrosis-related remodeling at the cellular level (Fig. 4I,J).

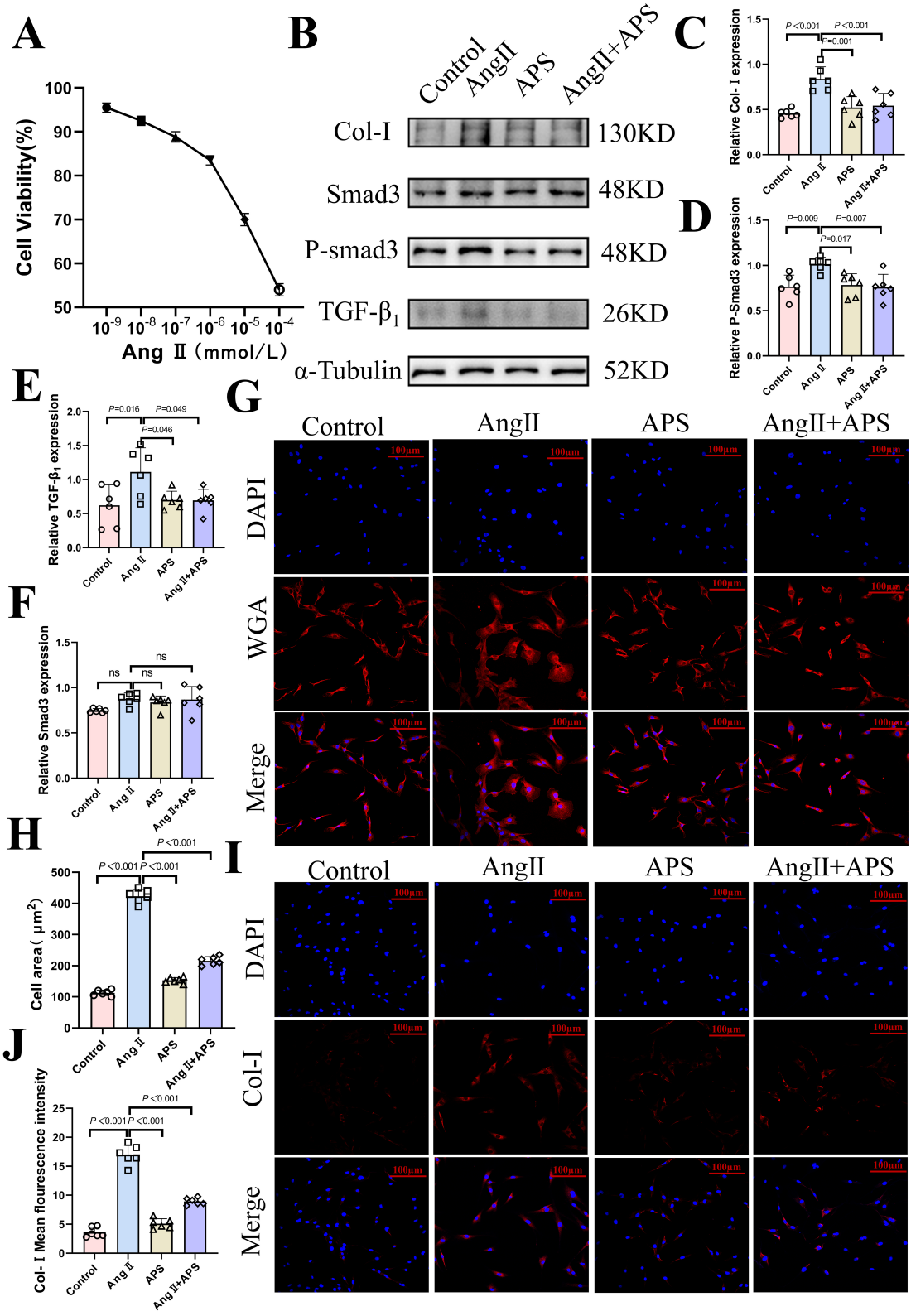

Fig. 4. APS suppresses angiotensin IIstimulated (Ang II)-induced hypertrophy in H9C2 cells. (A) Cell counting kit-8 (CCK8) assay of cell viability at different concentrations of Ang II. (B) Western blotting detecting the expression of TGF-β1, Smad3, p-Smad3, and Col-I in H9C2 cells. (C–F) Western blotting quantitative analysis. (G) Wheat Germ Agglutinin (WGA) staining, WGA (red) and DAPI (blue) representative ventricular immunofluorescence staining (scale bar = 100 μm). (H) Cell size analysis. (I) Col-I (red) and DAPI (blue) representative ventricular immunofluorescence staining (scale bar = 100 μm). (J) Col-I average fluorescence intensity analysis. ns, no statistical difference. n = 6.

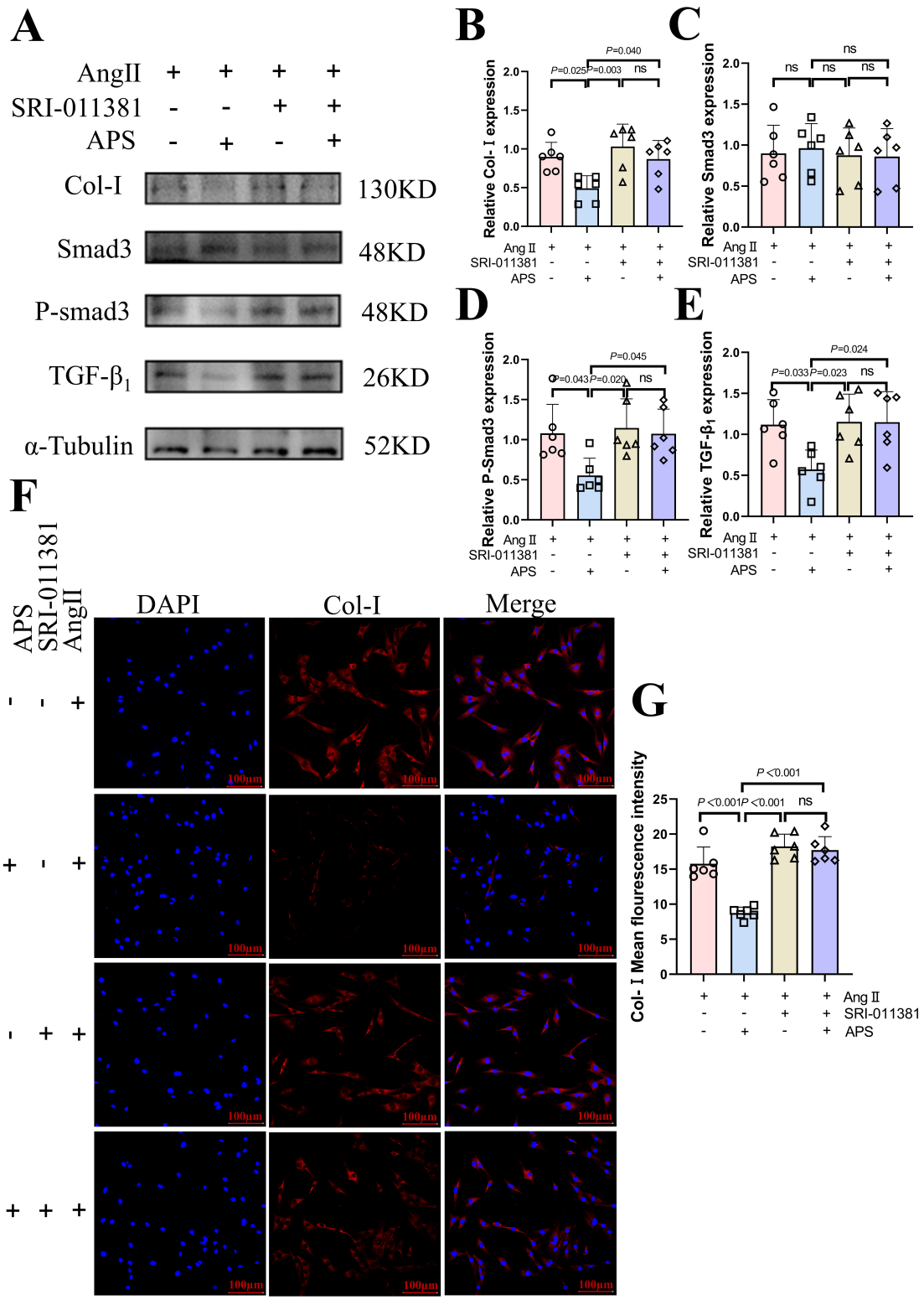

Fig. 5. APS exerts antifibrotic-Fibrotic effects via the TGF-β_1/Smad3 pathway. (A) Western blotting detecting the expression of TGF-β_1, Smad3, p-Smad3, and Col-I in H9C2 cells. (B–E) Western blotting quantitative analysis. (F) Col-I (red) and DAPI (blue) representative ventricular immunofluorescence staining (scale bar = 100 μm). (G) Col-I average fluorescence intensity analysis. ns, no statistical difference. n = 6.

3.5 Antifibrotic Effects of APS Depend on TGF-β_1/Smad3 Pathway Inhibition

To further confirm pathway specificity, Ang II-stimulated cells were co-incubated with the TGF-β_1/Smad3 agonist SRI-011381. This intervention enhanced TGF-β_1, p-Smad3, and Col-I expression and abolished the inhibitory effects of APS. Similarly, the reduction of Col-I fluorescence intensity by APS was no longer evident in the presence of the agonist. These results strongly support the conclusion that APS-mediated suppression of myocardial fibrosis relies on regulation of the TGF-β_1/Smad3 signaling cascade (Fig. 5A–G).

4. Discussion

HCM is the most common genetic heart disorder and continues to pose a major challenge to cardiovascular health worldwide [15]. A key feature of HCM pathophysiology is maladaptive cardiac remodeling, characterized by myocyte hypertrophy, interstitial fibrosis, and microvascular dysfunction [3]. Myocardial fibrosis plays a crucial role in disrupting normal cardiac structure and function, contributing to impaired diastolic and systolic performance, and increasing the risk of arrhythmias [16]. Furthermore, myocardial fibrosis is strongly associated with adverse clinical outcomes, including sudden cardiac death. Therefore, targeting myocardial fibrosis has become a promising therapeutic strategy in the management of HCM [17].

Among diverse antifibrotic strategies, traditional Chinese medicine has demonstrated unique advantages due to its multi-target and holistic regulatory properties. *Astragalus membranaceus*, a widely used Qi-tonifying herb in clinical practice, contains major active components such as astragaloside IV and APS [18,19]. As a natural polysaccharide, APS exerts diverse pharmacological effects, including antioxidant, anti-apoptotic, anti-inflammatory, and immunomodulatory activities [20]. Recent studies have shown that APS plays important roles in attenuating fibrosis across multiple organs. For instance, APS significantly suppresses isoproterenol-induced myocardial hypertrophy and improves cardiomyocyte morphology [21]. In renal fibrosis models, APS reduces ECM deposition by inhibiting the TGF-β_1/mitogen-activated protein kinase (TGF-β_1/MAPK) pathway [22]. In hepatic fibrosis, it attenuates disease progression via inhibition of the toll-like receptor 4/nuclear factor-κB (TLR4/NF-κB) pathway [23]; and in pulmonary fibrosis, APS reduces ECM accumulation and inflammation by regulating the phosphatidylinositol 3 kinase/protein kinase B (PI3K/AKT) pathway [24]. Collectively, these findings suggest that APS possesses broad-spectrum antifibrotic potential.

In the present study, we employed a TAC mouse model to mimic pressure overload-induced HCM. Echocardiographic analysis revealed that HCM mice exhibited significantly increased LAD, LVIDd, and LVIDs, along with reduced LVEF and LVFS, reflecting ventricular dilation and impaired contractile function—typical features of HCM. Pathological examination further demonstrated elevated Col-I expression and extensive collagen fiber deposition, confirming pronounced myocardial fibrosis. These findings underscore the central role of fibrosis in TAC-induced HCM.

Mechanistically, the TGF-β_1/Smad3 signaling axis is widely recognized as a pivotal driver of fibrotic processes in multiple organs [25]. Aberrant activation of TGF-β_1 promotes Smad3 phosphorylation and nuclear translocation, thereby upregulating pro-fibrotic genes such as Col-I, Col-III, and fibronectin. This cascade accelerates fibroblast-to-myofibroblast differentiation and ECM accumulation, exacerbating pathological remodeling [26]. Our study demonstrated that APS treatment significantly downregulated TGF-β_1 expression and Smad3 phosphorylation in the myocardium of TAC mice, with similar results observed in Ang II-induced H9C2 cells. Importantly, when the TGF-β_1/Smad3 pathway agonist SRI-011381 was applied, the inhibitory effects of APS on TGF-β_1, Smad3, and Col-I expression were largely abolished, indicating that the antifibrotic effects of APS are indeed mediated through suppression of the TGF-β_1/Smad3 pathway. These results clarify the mechanistic basis of APS activity and strengthen its translational potential in clinical practice.

The significance of this study lies in providing both systemic and molecular evidence that APS exerts protective effects against HCM by alleviating myocardial fibrosis via TGF-β_1/Smad3 inhibition. With the growing prevalence of HCM, standard pharmacological therapies (e.g., angiotensin converting enzyme inhibitors/angiotensin receptor blockers and β-blockers) have shown remarkable efficacy in delaying disease progression [27]. However, their direct antifibrotic effects remain limited. Therefore, novel therapeutic approaches targeting fibrosis are of great clinical importance. As a naturally derived polysaccharide with favorable safety profiles, APS holds promise as a novel candidate agent for the comprehensive management of HCM.

Nevertheless, several limitations of this study should be acknowledged. First, TAC mice and H9C2 cardiomyoblasts may not fully replicate the complex pathophysiology of human HCM. Validation studies using primary human cardiac fibroblasts and large animal HCM models are essential to confirm translational relevance. Second, the long-term safety, pharmacokinetics, and potential off-target effects of APS require systematic evaluation. Third, although this study confirmed that the antifibrotic effects of APS are dependent on the TGF-β_1/Smad3 pathway, it is possible that APS may also modulate other signaling pathways through crosstalk mechanisms. Future investigations employing multi-omics approaches and network analyses will be necessary to fully elucidate the pleiotropic mechanisms of APS.

5. Conclusions

Myocardial fibrosis is a major pathological manifestation of HCM. APS may effectively ameliorate HCM by suppressing myocardial fibrosis through modulation of the TGF-β_1/Smad3 signaling pathway.

Availability of Data and Materials

The datasets used and analyzed during the current study are available from the corresponding author on reasonable request.

Author Contributions

NNQ, WJW and BYL were responsible for study conception and design. BYL performed the data analysis and interpretation. WJW and NNQ drafted the manuscript. All authors contributed to editorial changes in the manuscript. All authors read and approved the final manuscript. All authors have participated sufficiently in the work and agreed to be accountable for all aspects of the work.

Ethics Approval and Consent to Participate

The study was conducted in accordance with the ARRIVE Guidelines The research protocol was approved by the Ethics Committee of Animal Ethics Committee of the General Hospital of the Northern Theater Command (Ethic Approval Number: 2024-09).

Acknowledgment

We would like to express our gratitude to all those who helped me during the writing of this manuscript.

Funding

This research received no external funding.

Conflict of Interest

The authors declare no conflict of interest.

References

[1] Bazgir F, Nau J, Nakhaei-Rad S, Amin E, Wolf MJ, Saucerman JJ, *et al*. The Microenvironment of the Pathogenesis of Cardiac Hypertrophy. Cells. 2023; 12: 1780. https://doi.org/10.3390/cells12131780.

[2] Becker RC, Owens AP, 3rd, Sadayappan S. Tissue-level inflammation and ventricular remodeling in hypertrophic cardiomyopathy. Journal of Thrombosis and Thrombolysis. 2020; 49: 177–183. https://doi.org/10.1007/s11239-019-02026-1.

[3] Schlittler M, Pramstaller PP, Rossini A, De Bortoli M. Myocardial Fibrosis in Hypertrophic Cardiomyopathy: A Perspective from Fibroblasts. International Journal of Molecular Sciences. 2023; 24: 14845. https://doi.org/10.3390/ijms241914845.

[4] Skórka P, Piotrowski J, Bakinowska E, Kiełbowski K, Pawlik A. The Role of Signalling Pathways in Myocardial Fibrosis in Hypertrophic Cardiomyopathy. Reviews in Cardiovascular Medicine. 2025; 26: 27152. https://doi.org/10.31083/RCM27152.

[5] Ong CH, Tham CL, Harith HH, Firdaus N, Israf DA. TGF-β-induced fibrosis: A review on the underlying mechanism and potential therapeutic strategies. European Journal of Pharmacology. 2021; 911: 174510. https://doi.org/10.1016/j.ejphar.2021.174510.

[6] Bogdahn U, Hau P, Stockhammer G, Venkataramana NK, Mahapatra AK, Suri A, *et al*. Targeted therapy for high-grade glioma with the TGF-β2 inhibitor trabedersen: results of a randomized and controlled phase IIb study. Neuro-Oncology. 2011; 13: 132–142. https://doi.org/10.1093/neuonc/noq142.

[7] Demers J, Ton AT, Huynh F, Thibault S, Ducharme A, Paradis P, *et al*. Atrial Electrical Remodeling in Mice With Cardiac-Specific Overexpression of Angiotensin II Type 1 Receptor. Journal of the American Heart Association. 2022; 11: e023974. https://doi.org/10.1161/JAHA.121.023974.

[8] Li CX, Liu Y, Zhang YZ, Li JC, Lai J. Astragalus polysaccharide: a review of its immunomodulatory effect. Archives of Pharmacal Research. 2022; 45: 367–389. https://doi.org/10.1007/s12272-022-01393-3.

[9] Du X, Zhao B, Li J, Cao X, Diao M, Feng H, *et al*. Astragalus polysaccharides enhance immune responses of HBV DNA vaccination via promoting the dendritic cell maturation and suppressing Treg frequency in mice. International Immunopharmacology. 2012; 14: 463–470. https://doi.org/10.1016/j.intimp.2012.09.006.

[10] Chen W, Xia Y, Zhao X, Wang H, Chen W, Yu M, *et al*. The critical role of Astragalus polysaccharides for the improvement of PPARα-mediated lipotoxicity in diabetic cardiomyopathy. PLoS ONE. 2012; 7: e45541. https://doi.org/10.1371/journal.pone.0045541.

[11] Zhao L, Zhong Y, Liang J, Gao H, Tang N. Effect of Astragalus Polysaccharide on the Expression of VEGF and EGFR in Mice with Lewis Transplantable Lung Cancer. Journal of the College of Physicians and Surgeons–Pakistan. 2019; 29: 392–394. https://doi.org/10.29271/jcpsp.2019.04.392.

[12] Chen D, Wu Y, Zhang Y, Yang H, Xiao Q. Effects of Astragalus polysaccharide on the structure and function of skeletal muscle in D-galactose-induced C57BL/6J mice. American Journal of Translational Research. 2024; 16: 7983–7993. https://doi.org/10.62347/CQDL1155.

[13] Dai DF, Liu Y, Basisty N, Karunadharma P, Dastidar SG, Chiao YA, *et al*. Differential effects of various genetic mouse models of the mechanistic target of rapamycin complex I inhibition on heart failure. GeroScience. 2019; 41: 847–860. https://doi.org/10.1007/s11357-019-00119-6.

[14] Ommen SR, Mital S, Burke MA, Day SM, Deswal A, Elliott P, *et al*. 2020 AHA/ACC Guideline for the Diagnosis and Treatment of Patients With Hypertrophic Cardiomyopathy: Executive Summary: A Report of the American College of Cardiology/American Heart Association Joint Committee on Clinical Practice Guidelines. Circulation. 2020; 142: e533–e557. https://doi.org/10.1161/CIR.0000000000000938.

[15] Liu Y, Chen G, Yao Y, Jiang Y, Wen C, Wang W, *et al*. The role of CARMA3 in regulating fibrosis to prevent hypertrophic cardiomyopathy. Cell Death Discovery. 2025; 11: 429. https://doi.org/10.1038/s41420-025-02645-z.

[16] Moravsky G, Ofek E, Rakowski H, Butany J, Williams L, Ralph-Edwards A, *et al*. Myocardial fibrosis in hypertrophic cardiomyopathy: accurate reflection of histopathological findings by CMR. JACC. Cardiovascular Imaging. 2013; 6: 587–596. https://doi.org/10.1016/j.jcmg.2012.09.018.

[17] Zhang Z, Zhang F, Zhang M, Xue H, Fan L, Weng Y. The role of SMAD signaling in hypertrophic obstructive cardiomyopathy: an immunohistopathological study in pediatric and adult patients. Scientific Reports. 2023; 13: 3706. https://doi.org/10.1038/s41598-023-30776-9.

[18] Liu W, Zhang Y, Hu D, Huang L, Liu X, Lu Z. Oral Astragalus polysaccharide alleviates adenine-induced kidney injury by reg-

ulating gut microbiota-short-chain fatty acids-kidney G protein-coupled receptors axis. Renal Failure. 2024; 46: 2429693. https://doi.org/10.1080/0886022X.2024.2429693.

[19] Chen Z, Liu L, Gao C, Chen W, Vong CT, Yao P, *et al*. Astragali Radix (Huangqi): A promising edible immunomodulatory herbal medicine. Journal of Ethnopharmacology. 2020; 258: 112895. https://doi.org/10.1016/j.jep.2020.112895.

[20] Zhao M, Xiang J, Meng Y, Sun H, Yang W, Li Z, *et al*. Astragalus Polysaccharide Hydrogels with Drug-Carrying Super Self-Assembly from Natural Herbs Promote Wound Healing. ACS Nano. 2025; 19: 21571–21588. https://doi.org/10.1021/acsnano.5c03744.

[21] Yao T, Chen JM, Shen LE, Yu YS, Tang ZH, Zang GQ, *et al*. Astragalus polysaccharide alleviated hepatocyte senescence via autophagy pathway. The Kaohsiung Journal of Medical Sciences. 2022; 38: 457–468. https://doi.org/10.1002/kjm2.12495.

[22] Gong F, Qu R, Li Y, Lv Y, Dai J. *Astragalus Mongholicus*: A review of its anti-fibrosis properties. Frontiers in Pharmacology. 2022; 13: 976561. https://doi.org/10.3389/fphar.2022.976561.

[23] Wang W, Zhou H, Sen A, Zhang P, Yuan L, Zhou S. Recent Advances in the Mechanisms and Applications of *Astragalus* Polysaccharides in Liver Cancer Treatment: An Overview. Molecules. 2025; 30: 2792. https://doi.org/10.3390/molecules30132792.

[24] He Y, Zhao WJ, Yang ZC, Qin MM, Wang Q, Lin S. Protective effect of *Astragalus* polysaccharide on diabetic nephropathy: A systematic review and meta analysis reveals the efficacy and potential mechanisms. Biomedical Reports. 2025; 22: 85. https://doi.org/10.3892/br.2025.1963.

[25] Budi EH, Schaub JR, Decaris M, Turner S, Derynck R. TGF-β as a driver of fibrosis: physiological roles and therapeutic opportunities. The Journal of Pathology. 2021; 254: 358–373. https://doi.org/10.1002/path.5680.

[26] Meng L, Lu Y, Wang X, Cheng C, Xue F, Xie L, *et al*. NPRC deletion attenuates cardiac fibrosis in diabetic mice by activating PKA/PKG and inhibiting TGF-β1/Smad pathways. Science Advances. 2023; 9: eadd4222. https://doi.org/10.1126/sciadv.add4222.

[27] Ommen SR, Ho CY, Asif IM, Balaji S, Burke MA, Day SM, *et al*. 2024 AHA/ACC/AMSSM/HRS/PACES/SCMR Guideline for the Management of Hypertrophic Cardiomyopathy: A Report of the American Heart Association/American College of Cardiology Joint Committee on Clinical Practice Guidelines. Circulation. 2024; 149: e1239–e1311. https://doi.org/10.1161/CIR.0000000000001250.